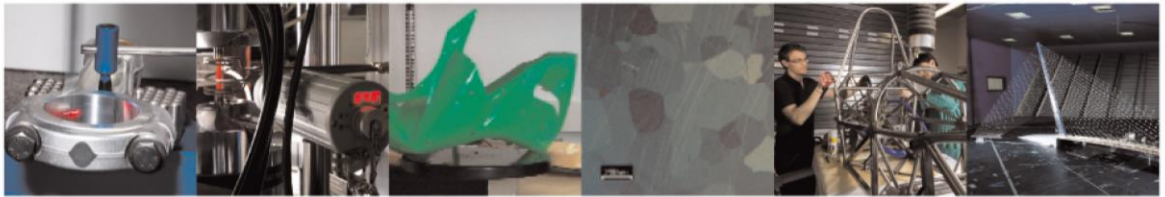




POLITECNICO  
MILANO 1863

DIPARTIMENTO DI MECCANICA



## Effect of in-source beam shaping and laser beam oscillation on the electromechanical properties of Ni-plated steel joints for e-vehicle battery manufacturing

Caprio, L.; Previtali, B.; Demir, A. G.

This article may be downloaded for personal use only. Any other use requires prior permission of the author and AIP Publishing. This article appeared in Leonardo Caprio, Barbara Previtali, Ali Gökhan Demir; Effect of in-source beam shaping and laser beam oscillation on the electromechanical properties of Ni-plated steel joints for e-vehicle battery manufacturing. J. Laser Appl. 1 November 2023; 35 (4): 042030 and may be found at <https://doi.org/10.2351/7.0001151>

This content is provided under [CC BY-NC-ND 4.0](https://creativecommons.org/licenses/by-nc-nd/4.0/) license



# EFFECT OF IN-SOURCE BEAM SHAPING AND LASER BEAM OSCILLATION ON THE ELECTRO-MECHANICAL PROPERTIES OF NI-PLATED STEEL JOINTS FOR E-VEHICLE BATTERY MANUFACTURING

# 0784\_1173\_000134

Leonardo Caprio<sup>1</sup>, Barbara Previtali<sup>1</sup>, Ali Gökhan Demir<sup>1</sup>

<sup>1</sup> Department of Mechanical Engineering, Politecnico di Milano, Via Giuseppe La Masa 1, Milano, Italy

## Abstract

Laser welding is a key enabling technology the transition towards electric mobility, producing joints with elevated electrical and mechanical properties. In the production of battery packs, cell to busbar connections are challenging due to the strict tolerances and zero-fault policy. Hence, it is of great interest to investigate how beam shaping techniques may be exploited to enhance the electro-mechanical properties as well as improve material processability. Industrial laser systems often provide the possibility to oscillate dynamically the beam or redistribute the power in multi-core fibers. Although contemporary equipment enables elevated flexibility in terms of power redistribution, further studies are required to indicate the most adequate solution for the production of high performance batteries.

Within the present investigation, both in-source beam shaping and beam oscillation techniques have been exploited to perform 0.2-0.2 mm Ni-plated steel welds in lap joint configuration, representative of typical cell to busbar connections. An experimental campaign allowed to define process feasibility conditions where partial penetration welds could be achieved by means of in-source beam shaping. Hence, beam oscillation was explored to perform the connections. In the subset of feasible conditions, the mechanical strength was determined via tensile tests alongside electrical resistance measurements. Linear welds with a Gaussian beam profile enabled joints with the highest productivity at constant electro-mechanical properties. Spatter formation due to keyhole instabilities could be avoided by redistributing the emission power via multi-core fibers whilst dynamic oscillation did not provide significant benefits.

## Introduction

The electric mobility sector is focusing on the development of highly efficient battery systems to provide competitive solutions with respect to internal combustion engines. In order to obtain the desired voltage, capacity and current rating of battery packs

multiple cells need to be connected in series and parallel and different joining technologies may be employed [1–3]. Currently, Li-based batteries are the reference solution for the realisation of high performance battery packs [4]. Li-based batteries are typically realised in different form factors (namely cylindrical, pouch and prismatic cells)[5]. Different joining solutions have been explored throughout the scientific and industrial communities for the realisation of cell to busbar connections in order to manufacture operational battery packs. The selection of the technological process often relies on a compromise between the applicability, performance, capital cost and productivity of the available solutions for a specific geometry. For instance, ultrasonic welding processes may be exploited for the joining of pouch or prismatic cells but are less apt for the joining of cylindrical cells [6]. Analogously bolted connections may be applicable for connecting prismatic cell connectors [7] whilst they result in excessive incumbrance for the realisation of battery packs composed by multiple cylindrical cells [8].

The present investigation focuses on evaluating novel beam shaping solutions for the laser of Li-ion cylindrical cells. The connection between these cells is typically performed by either Resistance Spot Welding (RSW) or laser welding. RSW has become a popular solution given its simple applicability and low cost [9,10]. Moreover, it possesses the significant advantage of ensuring the absence of gap between the welding electrodes and the two sheets being contacted given the intrinsic necessity of applying a pressure to perform the joining operation. On the other hand, the non-contact nature of the laser welding process provides the advantage of higher productivity whilst avoiding tool wear. Laser welding is becoming the reference technique for the production of battery packs with Li-ion cylindrical cells. For instance, Brand *et al.* demonstrated that laser welding can realise connections with the highest performance in terms of mechanical and electrical properties for CuZn37 busbar connections to 26650 Li-ion cells [11].

Concurrently, state of the art laser welding systems propose innovative solutions which can be appealing

process solutions although demonstrative studies are required to disclose their actual impact. For instance, novel generation laser sources emitting in the blue and green wavelengths are promising for the realisation of laser welded connections of thin sheet materials highly reflective to conventional near-infrared laser radiation [12,13].

Within the industrial and scientific communities there is a strong interest towards the use of beam shaping techniques to modify the power spatial distribution. In particular, two of the most commonly examined approaches are dynamic oscillation of the laser beam or in-source beam shaping via the use of multi-core fibers. Dynamic beam oscillation relies on high frequency motion of the laser beam superimposed to the translation direction of the weld trajectory. In-source beam shaping may be achieved within the laser source by allocating the laser emission to different transport fibers positioned coaxially such that the spatial emission profile corresponds to the superposition of a Gaussian beam (transported in the inner core) and ring mode (via the outer core). For instance, Schmidt *et al.* provided a comprehensive analysis regarding laser welding of Al/Cu in lap joint configuration indicating that dynamic beam oscillation can help to enlarge the weld seam thus reducing the electrical resistance [14]. Punzel *et al.* exploited multi-core fiber to reduce porosity formation during the welding of different Al-alloys [15]. Prieto *et al.* and Sun *et al.* also investigated the tailoring of the power distribution for the welding of Al for e-mobility applications [16,17]. Chianese *et al.* explored beam oscillation for the joining of copper to steel joints whilst Rinne *et al.* exploited in-source beam shaping [18,19].

Even though there has been significant attention towards the use of such techniques, a comprehensive study is required to understand the effects over the electrical characteristics of laser welded joints. Often, research has focused on the enabling aspects of beam shaping solutions whilst open questions remain with regards to which approach is more convenient in terms of the electro-mechanical properties of the joints.

The redistribution of the emission power with the use of dynamic beam oscillation or the use of multi-core fibers may allow to achieve joints with a larger seam width, possibly suppressing the spatter formation and allowing for a more tolerant process in terms of penetration depth. There is evidence within the scientific literature that beam shaping techniques may improve the mechanical and electrical properties of the joints. For instance, Schmidt *et al.* demonstrated an inversely proportional correlation between the

connection area (represented by the interface width) and the electrical resistance of Al/Al, Al/Cu and Cu/Cu joints[14]. With regards to the resistance of Al/Al lap joint, Sun *et al.* showed that an increase in the amplitude of the laser beam oscillation yields an increase of the interface width which is directly proportional to the weld strength[20]. Hence, it can be expected that the use of beam shaping techniques may be exploited to tailor the weld geometry in order to improve the electro-mechanical properties of joints.

Specifically for e-mobility applications the combined use of in-source beam shaping with dynamic beam oscillation has not yet been assessed. Hence, the aim of the current investigation is to disclose the effect of in-source and dynamic beam oscillation over the electro-mechanical properties for the welding of thin Ni-plated steel sheets in lap-joint configuration. This joint configuration simulates typical solution employed to connect Li-ion cylindrical cells and a busbar and requires a partial penetration connection to avoid electrolyte expulsion. A flexible welding system with a multi-core fiber laser enabling both in-source and dynamic beam shaping was employed to explore the process feasibility window with both techniques. Having defined stable processing conditions, a second part of the study focused on the definition of the electrical resistance of the connections as well its mechanical strength, comparing the novel solutions also with conventional resistance spot welded (RSW) connections.

## Materials & method

### Material and joint geometry

The scope of the present work consisted in determining the mechanical and electrical properties of cell to busbar connections exploiting novel solutions for the laser welding process. For such reason the welding of two Ni-plated steel sheets of 0.2 mm thickness in lap joint configuration was performed with different welding systems, where the lower sheet simulated the cell casing whilst the upper material represented the sheet typically employed to connect in series and parallel the different cells. The material employed for the current investigation was a 0.2 mm thick Ni-plated steel sheet specifically designed for the realization of cell casings and connectors (Hilumin, Tata Steel Europe, London, United Kingdom).

### Welding systems

A remote fiber laser welding system which enabled both in-source and dynamic beam shaping of the laser emission. The system was composed of a laser source which could redistribute the emission power between

an inner core and an outer core of the transport fiber (nLIGHT, AFX1000, Vancouver, Washington, USA). The main specifications of the laser welding set up are reported in Table 1.

Table 1. Main specifications of the laser welding system

Parameter	Value
Emission wavelength, $\lambda$	1070 nm
Focal length of collimator, $f_{col}$	60 mm
Inner fibre core diameter, $d_{core,inner}$	14 $\mu\text{m}$
External fibre core diameter, $d_{core,ext}$	40 $\mu\text{m}$
Maximum power inner core, $P_{max,inner}$	600 W
Maximum power outer core, $P_{max,outer}$	1200 W
BPP inner beam, $BPP_{inner}$ (mm · mrad)	0.48
BPP outer beam, $BPP_{outer}$ (mm · mrad)	2.19
Beam waist diameter with BS0, $d_{0,BS0}$	70 $\mu\text{m}$
Beam waist diameter with BS6, $d_{0,BS6}$	200 $\mu\text{m}$

The inner core of the laser system corresponded to 14  $\mu\text{m}$  whilst the outer core to 40  $\mu\text{m}$ . The inner core could transport up to 600 W of laser emission power whereas the outer core could exploit the maximum emission power of the laser source corresponding to 1200 W. The laser beam exiting the transport fiber exhibited a Beam Parameter Product of 0.41 mm·mrad whereas the BPP of the beam emitted from the outer core corresponded to 2.10 mm·mrad. The process light was launched into a scanner head (AM module, Raylase, Wessling, Germany) via a collimating unit with a focal length of 60 mm.

Prior to the deflection by means of two galvanometric mirrors, the laser light was focused by two optical elements consisting in a fixed focusing lens and a fast moving lens in the Z direction which allowed to compensate the focal position throughout the working plane. In the central position of the working field, theoretical calculations allowed to estimate the beam waist diameter emitted from the inner single mode core at 70  $\mu\text{m}$ . In the case the laser light was emitted from the outer core the beam waist diameter was calculated at 200  $\mu\text{m}$ . The light propagation path is reported schematically in Figure 1.

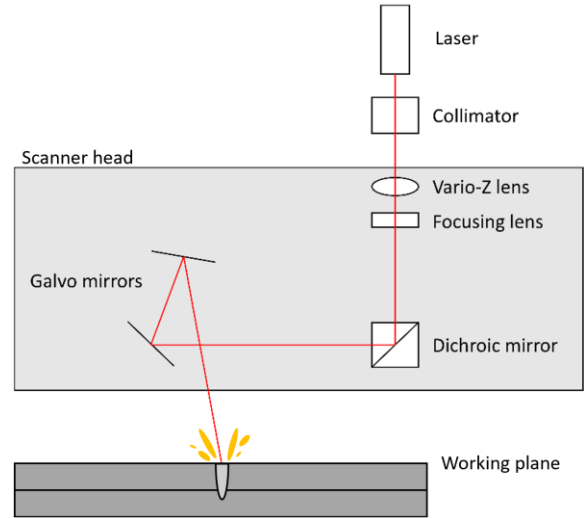


Figure 1. Schematic representation of the optical propagation path of the laser beam with the principal optical components of the remote welding system.

The laser emission power could be flexibly redistributed between the inner and outer core of the transport fiber. In order to indicate synthetically the power ratio distribution between the inner and outer core the terminology Beam Shape,  $BS_i$  where the subscript  $i$  indicates a ratio in the distribution of the laser power from the inner towards the outer core. The corresponding power distribution between the inner and outer core of the transport fiber for the various  $BS$  are reported in Figure 2. For instance,  $BS_2$  corresponds to a 60% of the total emission power delivered to the inner core whereas 40 % is instead delivered via the outer core. Moreover, Figure 2 shows the measurements of the spatial distribution of the emission power. The emission profiles were obtained by sampling the beam and exposing a CMOS camera sensor of a beam profiler Gentec Beamage Series USB 3.0, Quebec City, Canada) according to procedures described in a previous publication [21].

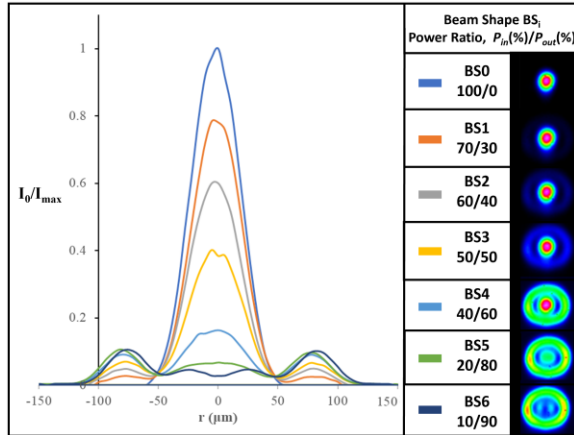


Figure 2. Spatial distribution of the emission power for the different Beam Shape indexes at different levels between the inner and outer core. The irradiance levels are reported with respect to the peak irradiance value.

In order to compare the performance of laser welded joints with conventional joining techniques, a resistance spot welding machine was employed namely Glitter 801D (Joyfay Int, Cleveland, USA). The energy grade of the spot welding process could be regulated via its electronic control system.

### Characterization

Specimen geometry was defined in accordance with the standard ISO 14274:2016 for tensile testing and was maintained constant throughout the experimental activities. The weld region was maintained at the center of the specimen whilst the other geometrical parameters are indicated in Figure 3 a). The same specimen geometry could be employed for the characterization of the electrical resistance of the joint. Tensile testing was conducted on a universal testing machine (Alliance RT 100, MTS, Eden Prairie, MN, USA) with 100 kN maximum force allowing to determine the Ultimate Tensile Force (UTF).

Non-destructive electrical testing was conducted by imposing a fixed value of current of 3 A at the extremity of the samples by means of a calibrated DC power supply (DP832, RIGOL, Beijing, China). The voltage difference was then sampled by means of a high resolution nanovoltmeter (8846A, Fluke, Everett, WA, USA). An internal calibration procedure was developed and allowed to estimate the measurement accuracy 0.4 μΩ. The connection scheme of the electrical measurement is shown in Figure 3 b) whilst the connection positions are indicated in Figure 3 a).

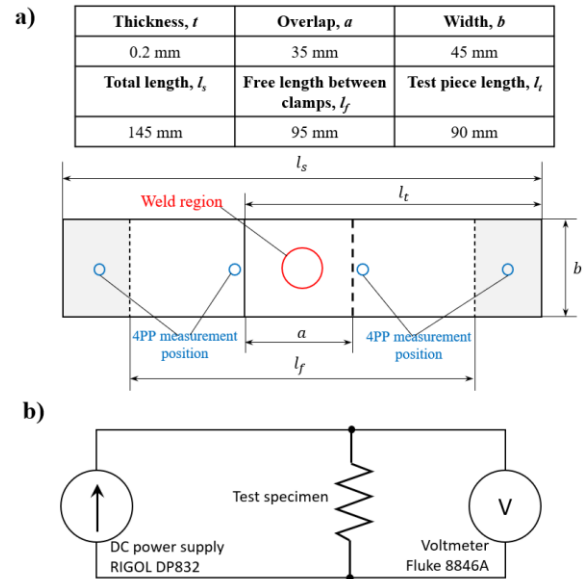


Figure 3. a) Specimen geometry and specifications and b) 4 point-probe (4PP) connection scheme for the measurement of the electrical resistance

Standard metallographic analyses were employed to disclose the melt region generated by the welding process. Procedures consisted in cutting the weld transversally to the advancement direction, encapsulating the samples in resin followed by mechanical grinding and polishing of the metal surface. Chemical etching with a 5% Nital solution allowed to observe the melt region that was acquired by means of an optical microscope (UM 300 I BD, EchoLAB, Paderno Dugnano, Italy). It was thus possible to measure the interface width of the joints which corresponds to the width of the weld seam at the interface between the two sheets.

### Experimental design to assess process feasibility

An experimental investigation was planned to determine the process feasibility by exploiting in-source and dynamic beam shaping solutions enabled by the laser welding system. A first qualitative assessment of the process was conducted by observing the cross-sectional metallographies of the weld seam allowing to determine processability regions for the realization of successful cell to busbar connections. The weld seam could thus be classified into three categories (shown schematically in Figure 4):

- No penetration: The weld seam does not penetrate the underlying sheet. This condition is undesirable due to the fact that the connection between the busbar and cell is not generated.

- Partial penetration: When the weld seam penetrates completely the first sheet and the only partially the second underlying sheet hence corresponding to a successful connection
- Full penetration: When the weld seam completely melts both the top and bottom sheet. This output is undesirable since it implies that the laser beam can interact with internal parts of the cell.

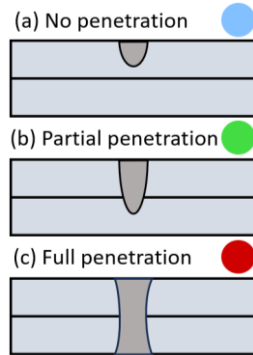


Figure 4. Schematic representation of the categorical characterisation of the process outcome.

The joint geometry and specimen design were maintained constant throughout all the investigation as previously presented. The connection consisted in a lap joint welding of two Ni-plated steel sheets with straight linear weld trajectory with a length of 20 mm representative of connection paths.

An initial experimental campaign was designed with a wide range of process parameters to determine the process feasibility window with in-source beam shaping. Four of the beam shape indexes (namely BS0, BS2, BS4 and BS6) were tested to investigate the effect of different spatial distribution over the process dynamics and outcome.

Table 2. Fixed and variable factors of the experimental design to assess the process feasibility of linear welds with in-source beam shaping

Fixed factors	
Focal position, $f$ (mm)	0
Trajectory	No oscillation
Variable factors	
Laser power, $P$ (W)	300; 450; 600; 750; 900; 1050; 1200
Speed, $v$ (mm/s)	100; 200; 300; 400; 500
Beam shape	BS0; BS2; BS4; BS6

Laser power was varied between 300 and 1200 W with seven levels, depending on the applicability with the tested beam shape. Tests at power levels above 600W and 750 W could not be conducted with BS0 and BS2 respectively due to power limitations on the inner core of the laser source. Five levels of weld speed from 100 to 500 mm/s were chosen. The fixed and variable factors of this design of experiments are reported in Table 2.

A second experimental campaign was designed to assess the combined effect of wobbling and in-source beam shaping over the joint outcome. The results were analyzed categorically to determine the operational range with such solutions. A full factorial experimental campaign was designed (reported in Table 3).

Table 3. Fixed and variable factors of the experimental design to assess the process feasibility conditions of linear welds with in-source beam shaping and wobbling

Fixed factors	
Focal position, $f$ (mm)	0
Trajectory	Circular wobble
Wobble frequency, $WF$ (Hz)	1000
Variable factors	
Laser power, $P$ (W)	300; 600; 900; 1200
Speed, $v$ (mm/s)	100; 200
Beam shape	BS0; BS2; BS4; BS6
Wobble amplitude, $WA$ (mm)	0.2; 0.3

The welds were performed in a more restricted selection of laser powers from 300 to 1200 W with four levels and employing the four beam shape distributions previously tested (BS0, BS2, BS4 and BS6). Two levels of weld speed ( $v=100; 200$  mm/s) and two levels of wobbling amplitude ( $WA= 0.2; 0.3$  mm) were used. The wobbling frequency was maintained constant at 1000 Hz.

#### Experimental design for the characterization of the electro-mechanical properties

Having defined the feasible conditions for partial penetration joints exploiting both in-source and dynamic beam shaping, an experimental campaign was designed to study the electro-mechanical properties. Experiments were performed in the conditions selected in the previous phase and replicated five times. As an added point of comparison iso-productivity conditions were also explored in this phase. Hence, beyond comparing the performance at

single joint level, by taking the less productive condition as a reference, multiple joints were performed with the higher productivity conditions until the productivity was matched. In practical terms if two welding conditions employed weld speeds of  $v$  and  $5v$ , the number of weld joints were 5 and 1 respectively to match the total welding time.

### Comparison with resistance spot welding

In the final part of the experimental work laser produced partially penetrating weld joint were compared to RSW welds using single and double joints. Figure 5 reports the schematical layout of different conditions tested. All the selected conditions were tested for their electrical resistance as well as their ultimate tensile force (UTF).

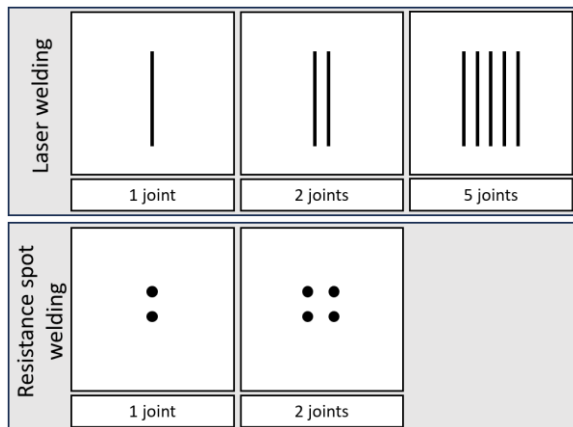


Figure 5. Layout of the joint geometry for the comparison of the electro-mechanical properties

## Results

### Process feasibility with in-source beam shaping

Figure 6 shows the processability map at different levels of the emission power for the various processing conditions. It is possible to observe that at a fixed level of emission power the Gaussian power distribution (BS0) allows to perform partial penetration joints at higher scanning velocities with respect to the doughnut shape (BS6). This effect is expected to be correlated to the reduction of the peak irradiance which is gradually reduced when redistributing the emission power from the inner towards the outer core. However, the use of higher levels of emission power with the doughnut beam shapes allows to achieve comparable levels in terms of productivity.

The selection of the conditions was made at the highest level of power where all beam shapes were available ( $P=600$  W) where partial penetration joints could be

achieved (indicated graphically by black circles in Figure 6).

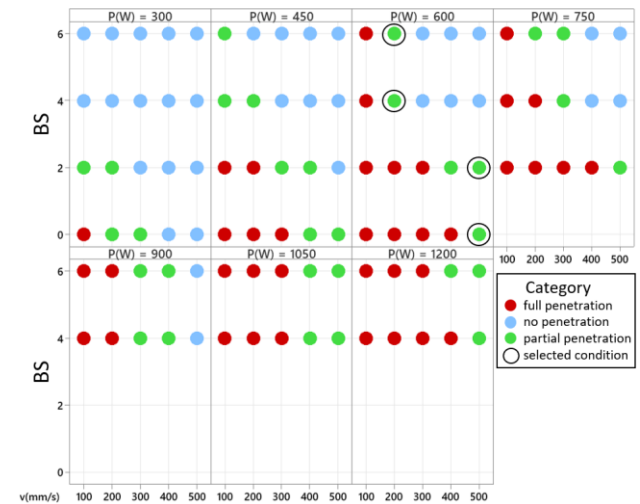


Figure 6. Process feasibility map for the lap welding of Ni-plated steel exploiting different in-source beam shaping profiles.

Representative metallographic cross-sections of these conditions are shown in Figure 7. Consistently to what may be expected, it is possible to observe that although similar penetration depths could be achieved, higher order beam shapes enabled a larger joint geometry.

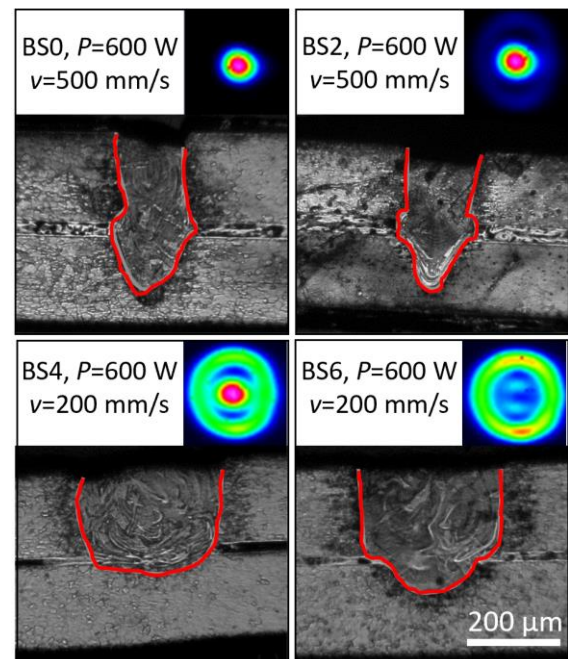


Figure 7. Metallographic cross-sections of the selected conditions when using in-source beam shaping. Red line indicates melt profile.

The weld bead shape obtained in such conditions exhibits a regular profile which is symptomatic of a more stable molten pool during the welding process, whilst BS0 and BS2 exhibit a narrow deep penetration weld geometry. Exploiting the outer ring of the fiber it was thus possible to regulate the aspect ratio of the joint geometry. Given the wide experimental design with single replicates it is difficult to draw conclusions regards the coupling efficiency of the process light with the feedstock material. However, it possible to observe that a larger beam diameter (BS4 or BS6) requires an increase in terms of the energy delivered to the material. However, considering that a greater amount of material is being melted in these conditions, it is possible to expect that a constant specific energy is required to process the material. Hence, an analytical model which may help to explain such effects is the lumped heat capacity model.

### Process feasibility with beam oscillation and in-source beam shaping

The second phase of the experimental investigation coupled the use of in-source shaping of the emission profile with dynamic oscillation of the laser beam. The process feasibility map with such techniques is reported in Figure 8.

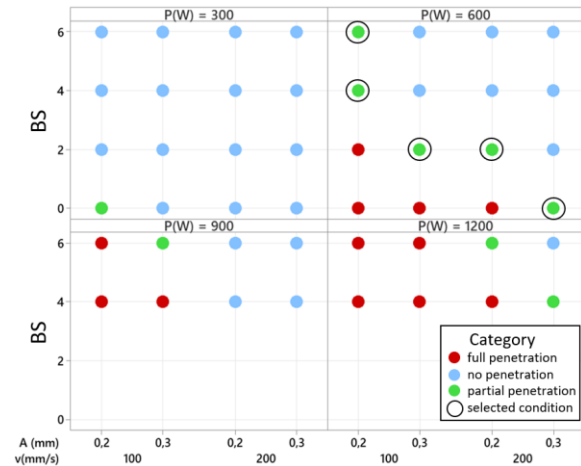


Figure 8. Process feasibility map for the lap welding of nickel plated steel with the use of dynamic beam oscillation combined with in-source beam shaping

In this case, process feasibility conditions were determined for different beam shape combinations for  $P=600$  W. Lower levels of power resulted in no penetration joints, whilst over penetration was achieved when employing higher levels of power and lower scan velocities. Once again, it appears that a specific energy density controls the melting behaviour of the material. Figure 9 shows the metallographic cross-sections of the joints. Beam oscillation allows to

enlarge the seam width also in the case of welds performed with the Gaussian BS0 as shown in Figure 9 (a). However, in order to obtain a partial penetration, joint the process productivity must be decreased with respect to linear welds for all beam shapes. However, the reduction in productivity when introducing beam oscillation is more contained in the case the outer ring is employed.

Once again, by doubling the emission power from the BS0 condition ( $P=600$  W,  $WA=0.3$ ) to BS6 ( $P=1200$  W,  $WA=0.2$ ) it is possible to obtain partial penetration welds with the same process velocity ( $v=200$  mm/s). Hence, this indicates that at equal levels of power a Gaussian beam is more efficient in performing a joint but this may be compensated by higher levels of emission power. On the other hand, lower peak irradiances are expected to generate less turbulent melt pools which can reduce spatter formation.

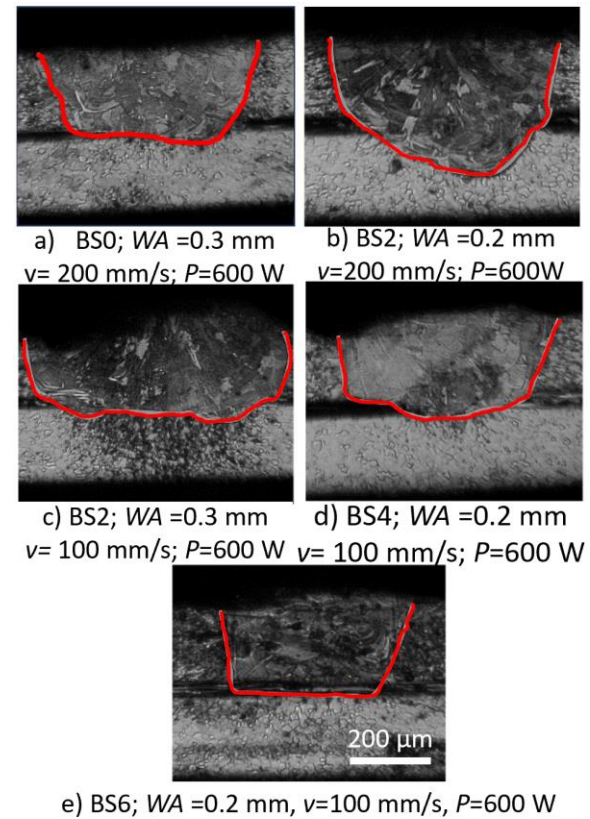


Figure 9. Metallographic cross-sections of selected conditions with beam oscillation. Red line indicates melt profile.

The conditions selected for the comparison in terms of electro-mechanical properties are reported graphically in Figure 8 and once again relate to the feasible combination of parameters capable of achieving partial penetration joints at a fixed level of emission power. Hence, in Table 4 the complete list of



conditions selected for the comparison of the electro-mechanical properties of the joints is resumed.

Table 4. List of conditions selected to perform partial penetration welds on 0.2 mm + 0.2 mm Ni-plated steel lap joints.  $P=600$  W for all conditions.

Beam shaping	BS	WA(mm)	v(mm/s)
None	0	-	500
In-source	2	-	500
In-source	4	-	200
In-source	6	-	200
Wobbling	0	0.3	200
In-source+Wobbling	2	0.2	200
In-source+Wobbling	2	0.3	100
In-source+Wobbling	4	0.2	100
In-source+Wobbling	6	0.2	100

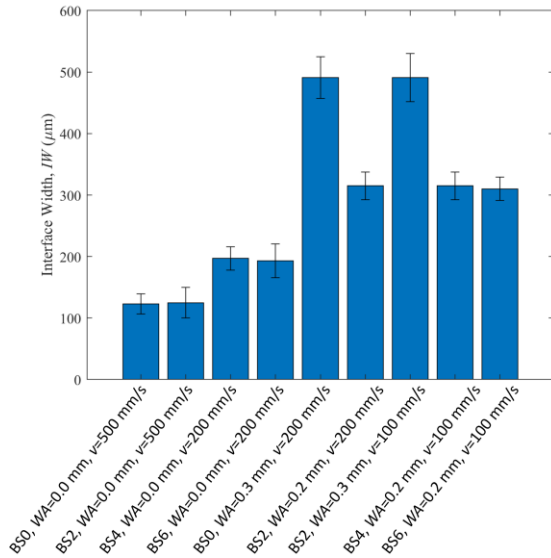


Figure 10. Interface width of the selected joints. Error bars are one standard deviation from the mean.

### Electrical and mechanical properties

Figure 11 a) reports the electrical resistance of the joints both for the single joint condition as well in iso-productivity situations where a greater number of weld lines was performed. In general, it is possible to observe that a single laser weld yields a lower electrical resistance with respect to a connection performed by Resistance Spot Welding. On the other hand, a double RSW joint allows to achieve comparable results. Overall, it is possible to observe

that non-significant differences appear between laser welded joints at a single joint level. The parameter which appears to affect most significantly the electrical resistance is the number of weld lines. However, given that larger weld seams obtained with doughnut beams or dynamic oscillation of the beam exhibit similar performance to narrow weld tracks performed with the gaussian beam shape, there is strong indication that the most significant factor impacting over the electro-mechanical performance is the actual joint trajectory. This is in accordance with observations by Schmidt *et al.* who indicated that the weld geometry can have significant impacts over the performance of electrical connections [11].

Figure 11 b) shows the ultimate tensile force of the joints as a function of the different process conditions. It can be observed that the mechanical properties exhibit inverse trends with respect to the electrical resistance previously discussed.

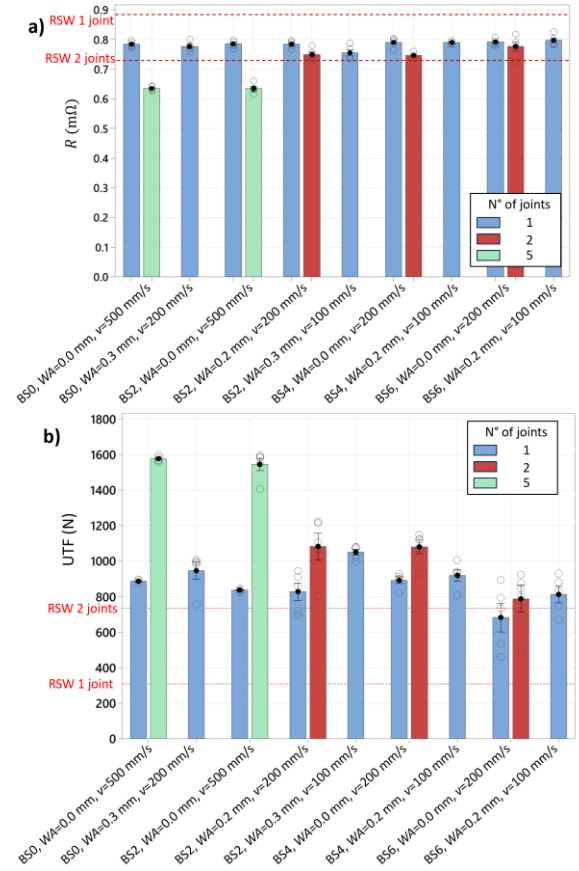


Figure 11. a) Electrical resistance and b) Ultimate Tensile Force of the joints. WA=0 indicates linear welds. Dashed red lines indicate electrical resistance of RSW joints. Error bars are one standard error from the mean.

Once again, the lower performance of RSW joints with respect to laser welded connections is confirmed. As mentioned in the introduction, the main reason to support this technology resides on the lower chance of faults due to its higher resilience to gap formation during the welding process. In case of linear welds the different beam shaping techniques did not yield statistically significant different results. Only conditions with large wobble amplitudes ( $WA=0.3$  mm) possess higher mechanical resistance. However, once again the most significant factor results being the geometry of the weld trajectory obtained in the iso-productivity conditions where Beam Shapes with elevated levels of irradiance (BS0 and BS2) were employed to perform multiple adjacent weld tracks.

In Figure 12 the mechanical strength and electrical resistance of the connections were correlated by a linear trend. A linear inverse relation can be observed indicating that a lower electrical resistance may be achieved when realizing connections with a higher mechanical strength. This result can be particularly appealing since it indicates that the mechanical strength of battery pack cell to busbar joints may be certified by testing the electrical resistance in a non-destructive manner.

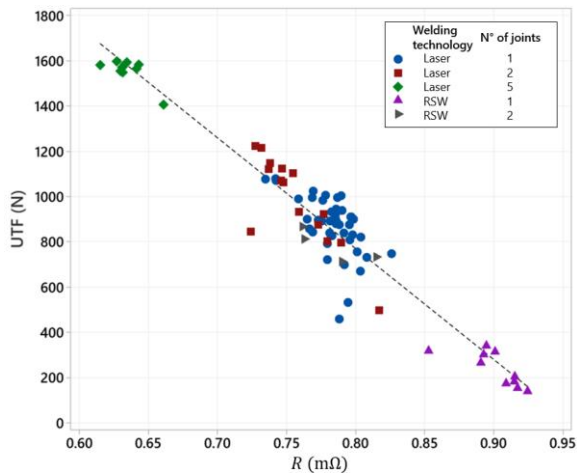


Figure 12. Ultimate Tensile Force UTF against electrical resistance R for the selected conditions categorized accordingly to the welding technology and the number of joints

## Discussion

Schimdt *et al.* indicated that the electrical resistance, is expected to be inversely correlated to the interface width[14]. Hence, redistributing the emission power to the outer core of the fiber was expected to yield joints with lower electrical resistance given the larger weld seams observable in Figure 7. Analogously, the use of spatial beam oscillation has the capability of enlarging

the width of the weld seam with respect to linear welds as demonstrated by the metallographic cross-sections of Figure 9. In the case of welding with dynamic beam oscillation, use of different power density distributions is not reflected by changes in the geometry of the weld seam, as shown in Figure 9 and the interface width measurements shown in Figure 10. However, a correlation between the interface width and the electrical resistance could not be determined in the present investigation. This is in accordance to results presented by Shaikh *et al.* during the welding of Cu-Hilumin where non-significant differences in terms of electrical resistance were found at varying levels of interface width[22]. Possibly this might be correlated to the fact that the superficial Nickel plating is the main current carrying vector in Hilumin (given its higher conductivity with respect to steel). Hence, the flow of electrons can be expected to act mostly superficially. Further studies analysing the material composition in the case of Hilumin-Hilumin joints may be required to disclose such effects, as well as comparative investigations with high current carrying materials such Al and Cu with tend to exhibit different behaviours as shown by Schmidt *et al.*[14]. Rather, the most significant factor resulted being the overall joint trajectory where multiple weld lines were capable of significantly reducing the overall electrical resistance as shown by the trend of Figure 12. This can be correlated also to the increase of the contact area between the two materials also in-between the weld regions where effects similar to a mechanical locking mechanism may be expected.

In general it must be considered that, higher levels of irradiance allow to achieve higher productivity. However, such effects can be easily compensated by the use of higher levels of emission power with doughnut shaped beams. An aspect which however has not been assessed in the present investigation is the contamination of the weld region due to spatter formation. This is a fundamental point in the development of industrial laser based joining solution for the e-mobility sector and requires greater attention. Given that there is evidence that different beam shaping techniques may have an effect from this perspective future works should also investigate these aspects [15].

The overall results show that oscillation and in-source dynamic beam shaping techniques can provide a wide range of seam geometries adaptable to different application needs. A generic first allocation of the used techniques can be made considering the results. Gaussian beams can be employed to exploit higher process speed for thicker sections or where the full penetration does not generate an issue. The use of in-

source beam shaping with ring beams can be exploited especially with cap to can and busbar to can connections, where limited penetration and a more stable keyhole is required. Wobbling can be exploited to potentially have a higher tolerance with gap formation. Future works will investigate the capacity of the beam shaping techniques to tolerate these defect types.

### Conclusions

This investigation explored the use of in-source and dynamic beam oscillation as spatial beam shaping techniques during the laser welding of Ni-plated sheets for electric mobility applications representing typical cylindrical cell to busbar connections. The experimental investigations designed allowed to determine process parameters for where successful partial penetration joints could be achieved. Finally, the selected conditions were characterized in terms of their electrical resistance and mechanical strength. Hence, it is possible to conclude that:

- At equal levels of emission power, higher productivity could be obtained with beams with higher levels of irradiance. However, comparable productivity levels could be achieved by means of doughnut shaped beams by increasing the emission power, allowing the realisation of connections with larger interface widths.
- The different beam shaping approaches did not yield statistically significant differences in terms of the electrical and mechanical properties at single joint level. On the other hand, the weld trajectory resulted being the most significant parameter.
- The mechanical resistance in terms of ultimate tensile force is correlated by an inverse linear relationship to the electrical resistance.

Future developments of the present research will be aimed at disclosing the effects of the different beam shaping techniques on the process dynamics via high speed imaging. Moreover, there is interest in assessing the effects beam shaping techniques at during the welding of dissimilar materials.

### Acknowledgements

Optoprim and nLIGHT are acknowledged for providing the laser source. The authors are thankful to Tata Steel for supplying the weld material and to Raylase for supporting the activities by providing the scanner head and controller card. The Italian Ministry of Education, University and Research is acknowledged for the support provided through the National Plan of Recovery and Resilience.

### References

- [1] Zwicker, M. F. R., Moghadam, M., Zhang, W., and Nielsen, C. V., 2020, "Automotive Battery Pack Manufacturing – A Review of Battery to Tab Joining," *Journal of Advanced Joining Processes*, **1**(November 2019), p. 100017.
- [2] Das, A., Li, D., Williams, D., and Greenwood, D., 2018, "Joining Technologies for Automotive Battery Systems Manufacturing," *World Electric Vehicle Journal*, **9**(2).
- [3] Lee, S. S., Kim, T. H., Hu, S. J., Cai, W. W., and Abell, J. A., 2010, "Joining Technologies for Automotive Lithium-Ion Battery Manufacturing: A Review," *International Manufacturing Science and Engineering Conference*, pp. 541–549.
- [4] Kwade, A., Haselrieder, W., Leithoff, R., Modlinger, A., Dietrich, F., and Droeder, K., 2018, "Current Status and Challenges for Automotive Battery Production Technologies," *Nat Energy*, **3**(4), pp. 290–300.
- [5] L bberding, H., Wessel, S., Offermanns, C., Kehrer, M., Rother, J., Heimes, H., and Kampker, A., 2020, "From Cell to Battery System in BEVs: Analysis of System Packing Efficiency and Cell Types," *World Electric Vehicle Journal*, **11**(4), pp. 1–15.
- [6] de Leon, M., and Shin, H. S., 2022, "Review of the Advancements in Aluminum and Copper Ultrasonic Welding in Electric Vehicles and Superconductor Applications," *J Mater Process Technol*, **307**.
- [7] Taheri, P., Hsieh, S., and Bahrami, M., 2011, "Investigating Electrical Contact Resistance Losses in Lithium-Ion Battery Assemblies for Hybrid and Electric Vehicles," *J Power Sources*, **196**(15), pp. 6525–6533.
- [8] Bolsinger, C., Zorn, M., and Birke, K. P., 2017, "Electrical Contact Resistance Measurements of Clamped Battery Cell Connectors for Cylindrical 18650 Battery Cells," *J Energy Storage*, **12**, pp. 29–36.
- [9] Phichai, N., Kaewtatip, P., Lailuck, V., Rompho, S., and Masomtob, M., 2019, "Parametric Effects of Resistance Spot Welding between Li-Ion Cylindrical Battery

- Cell and Nickel Conductor Strip,” *IOP Conference Series: Materials Science and Engineering*, Institute of Physics Publishing.
- [10] Godek, J., 2013, “Joining Lithium–Ion Batteries into Packs Using Small-Scale Resistance Spot Welding,” *Welding International*, **27**(8), pp. 616–622.
- [11] Brand, M. J., Schmidt, P. A., Zaeh, M. F., and Jossen, A., 2015, “Welding Techniques for Battery Cells and Resulting Electrical Contact Resistances,” *J Energy Storage*, **1**(1), pp. 7–14.
- [12] Zediker, M. S., Fritz, R. D., Finuf, M. J., and Pelaprat, J. M., 2020, “Laser Welding Components for Electric Vehicles with a High-Power Blue Laser System,” *J Laser Appl*, **32**(2), p. 022038.
- [13] Grabmann, S., Kriegler, J., Harst, F., Günter, F. J., and Zaeh, M. F., 2022, “Laser Welding of Current Collector Foil Stacks in Battery Production—Mechanical Properties of Joints Welded with a Green High-Power Disk Laser,” *International Journal of Advanced Manufacturing Technology*, **118**(7–8), pp. 2571–2586.
- [14] Schmidt, P. A., Schweier, M., and Zaeh, M. F., 2012, “Joining of Lithium-Ion Batteries Using Laser Beam Welding: Electrical Losses of Welded Aluminum and Copper Joints,” *ICALEO 2012 - 31st International Congress on Applications of Lasers and Electro-Optics*, **915**(2012), pp. 915–923.
- [15] Punzel, E., Hugger, F., Dinkelbach, T., and Bürger, A., 2020, “Influence of Power Distribution on Weld Seam Quality and Geometry in Laser Beam Welding of Aluminum Alloys,” *Procedia CIRP*, Elsevier B.V., pp. 601–604.
- [16] Prieto, C., Vaamonde, E., Diego-Vallejo, D., Jimenez, J., Urbach, B., Vidne, Y., and Shekel, E., 2020, “Dynamic Laser Beam Shaping for Laser Aluminium Welding in E-Mobility Applications,” *Procedia CIRP*, Elsevier B.V., pp. 596–600.
- [17] Sun, T., Franciosa, P., Sokolov, M., and Ceglarek, D., 2020, “Challenges and Opportunities in Laser Welding of 6xxx High Strength Aluminium Extrusions in Automotive Battery Tray Construction,” *Procedia CIRP*, **94**, pp. 565–570.
- [18] Chianese, G., Jabar, S., Franciosa, P., Ceglarek, D., and Patalano, S., 2022, “A Multi-Physics CFD Study on the Part-to-Part Gap during Remote Laser Welding of Copper-to-Steel Battery Tab Connectors with Beam Wobbling,” *Procedia CIRP*, Elsevier B.V., pp. 484–489.
- [19] Rinne, J. S., Nothdurft, S., Hermsdorf, J., Kaierle, S., and Overmeyer, L., 2020, “Advantages of Adjustable Intensity Profiles for Laser Beam Welding of Steel Copper Dissimilar Joints,” *Procedia CIRP*, **94**, pp. 661–665.
- [20] Sun, T., Mohan, A., Liu, C., Franciosa, P., and Ceglarek, D., 2022, “The Impact of Adjustable-Ring-Mode (ARM) Laser Beam on the Microstructure and Mechanical Performance in Remote Laser Welding of High Strength Aluminium Alloys,” *Journal of Materials Research and Technology*, **21**, pp. 2247–2261.
- [21] Galbusera, F., Caprio, L., Previtali, B., and Demir, A. G., 2023, “The Influence of Novel Beam Shapes on Melt Pool Shape and Mechanical Properties of LPBF Produced Al-Alloy,” *J Manuf Process*, **85**, pp. 1024–1036.

### Meet the authors

Leonardo Caprio is assistant professor at the Department of Mechanical Engineering of the Politecnico di Milano. His research activities focus on the development of laser-based processes for the e-Mobility sector and Industry 4.0.

Barbara Previtali in 2016 was appointed as Full Professor in the Mechanical Engineering Department, Politecnico di Milano. She leads the Sitec — Laboratory for Laser Applications and PromozioneL@ser with AITeM, which collects Italian laser users in industry and academia. Her current research interests include modeling, optimization and control of laser processes in their application in various fields. On these research subjects, she has authored or coauthored over 100 papers in refereed international journals and international conferences and two international patents

Ali Gökhan Demir completed his PhD in Mechanical Engineering at the Politecnico di Milano in

collaboration with the University of Cambridge in 2014. He has been an Associate Professor with the Department of Mechanical Engineering, Politecnico di Milano, since 2021. He leads LaserEMobility section of AITeM dedicated to the development of laser processes for eV manufacturing. His research interests include laser-based manufacturing processes with an emphasis to the light-material interaction mechanism in temporal, spatial and wavelength domains.